

On the Branching in the Emission Relations of Ca II lines in Solar Prominences

G. Stellmacher¹ and E. Wiehr²

¹ *Institute d'Astrophysique, Paris, France, email: stell@iap.fr*

² *Institut für Astrophysik, Göttingen, Germany, email: ewiehr@astro.physik.uni-goettingen.de*

Abstract. Spatially well resolved spectra of the emission lines Ca II K, Ca II 8542 and H β are analyzed in solar prominences. It is confirmed that the branching in the emission relations of Ca II versus H β correlates with the magnitude of non-thermal (turbulent) broadening.

Keywords: Prominences, Quiescent, Ca II emission, branching

1. Introduction

High precision spectroscopy of spatially and spectrally well resolved emission lines in quiescent prominences indicates that the simple concept of an average state for prominence matter can only be considered as a first-order approximation. The ratio of the integrated line intensity ('radiance') $E(He D_3)/E(H\alpha)$ and $E(He D_3)/E(H\beta)$ shows a noticeable increase in fainter (outer) parts of prominences.

Other examples are the significant differences ('branching') in the relations (a) of the radiance $E(Ca II K)$ vs $E(Ca II 8542)$ found by Landman and Illing (1977); (b) of the radiance $E(Ca II K, H)$ vs $E(H\alpha, \beta)$ found by Stellmacher (1978); and (c) of the central line intensity $I_0(Ca II K)$ vs $I_0(H\alpha)$ found by Engvold (1978).

The branching in the Ca II H&K radiance is accompanied by a concomitant variation of the widths of the Balmer lines relative to those of the Ca II H&K lines (Stellmacher 1979). It has been conjectured whether magnetic field coupling may produce selective non-thermal broadening of the Ca ions. However, such an effect was not found in the analysis by Landman et al. (1977).

In the present work we discuss the branching in the emission relations of Ca II K on the basis of new observations of the three emission lines Ca II K, H β , and Ca II 8542 ('IR'), obtained at good spatial and spectral resolution.

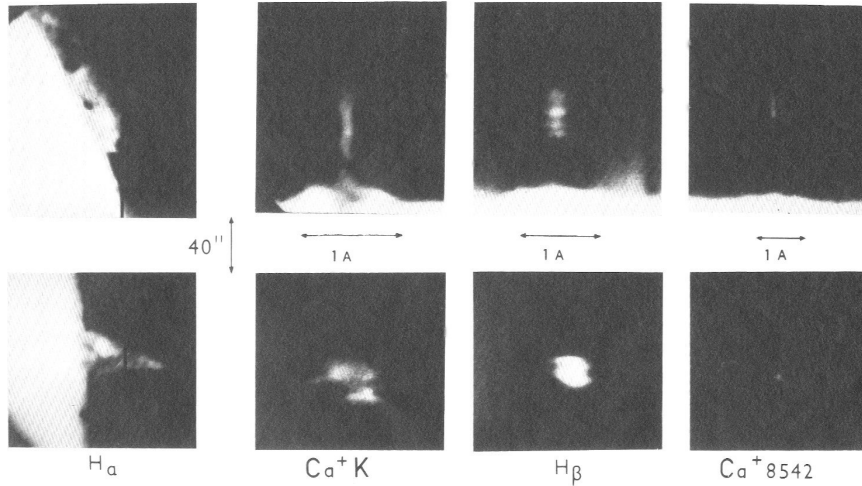


Figure 1. Two examples of observed data sets with $H\alpha$ slit-yaw images (*left panels*) and spectra of $Ca\ II\ K$, $H\beta$ and $Ca\ II\ IR$. Prominence $E\ 40^\circ N$ (*upper*) and $W\ 65^\circ N$ (*lower row*).

2. Observations

A set of spectra of the three lines was obtained photographically using a new type of proximity focused image intensifier (PROXITRONIC, Germany; single-stage) in the focal plane of the Czerny-Turner spectrograph at the Locarno station of the Göttingen Observatory (cf. Wiehr et al, 1980). The linear dispersion amounts to 0.115, 0.145, and 0.227 $\text{\AA}/\text{mm}$ for $Ca\ II\ K$, $H\beta$ and $Ca\ II\ IR$, respectively.

Table I. Obs. time, heliogr. position and max. of $H\beta$ radiance [$10^4\ \text{erg}/(\text{s cm}^2\ \text{ster})$] for the prominences observed on July 18, 1979.

09:00	east limb, $40^\circ N$	2.65
09:27	west limb, $45^\circ S$	0.89
12:20	west limb, $65^\circ S$	5.01
12:40	east limb, $05^\circ N$	5.28
12:50	east limb, $05^\circ S$	9.71

The spectra were taken with an exposure time of $\leq 60\ \text{sec}$ for the two $Ca\ II$ lines, while the typical exposure time for $H\beta$ was $\approx 12\ \text{sec}$; a total set of the three lines was obtained in $\approx 2.5\ \text{min}$. $H\alpha$ slit-jaw images were taken for each set of spectra on Kodak SO-392 film. A slit width of $150\ \mu$ was used, corresponding to a spatial resolution of 1.24 arcsec.

For the photometric calibration of the spectra we placed a wedge in front of the entrance slit, illuminated by a (de-focused) quiet region at disk-center. The absolute prominence emission was deduced from disk-center spectra calibrated with the reference continua given by Labs and Neckel (1968). For the K-line we used the value of 0.82 given by White and Suemoto (1968) for $\lambda = 3954.2 \text{ \AA}$ relative to an assumed continuum window at $\lambda = 3999.9 \text{ \AA}$.

The micro-photometry was performed with the photometer of the Institut d'Astrophysique de Paris (Brückner 1961). The properly scaled scattered-light intensity-profiles were subtracted from each scan of the prominence emission lines. All spectra were observed on July 18, 1979, a day with stable seeing conditions. The observed prominences are listed in Table 1. Two examples of a complete set of emission spectra are shown in Figure 1.

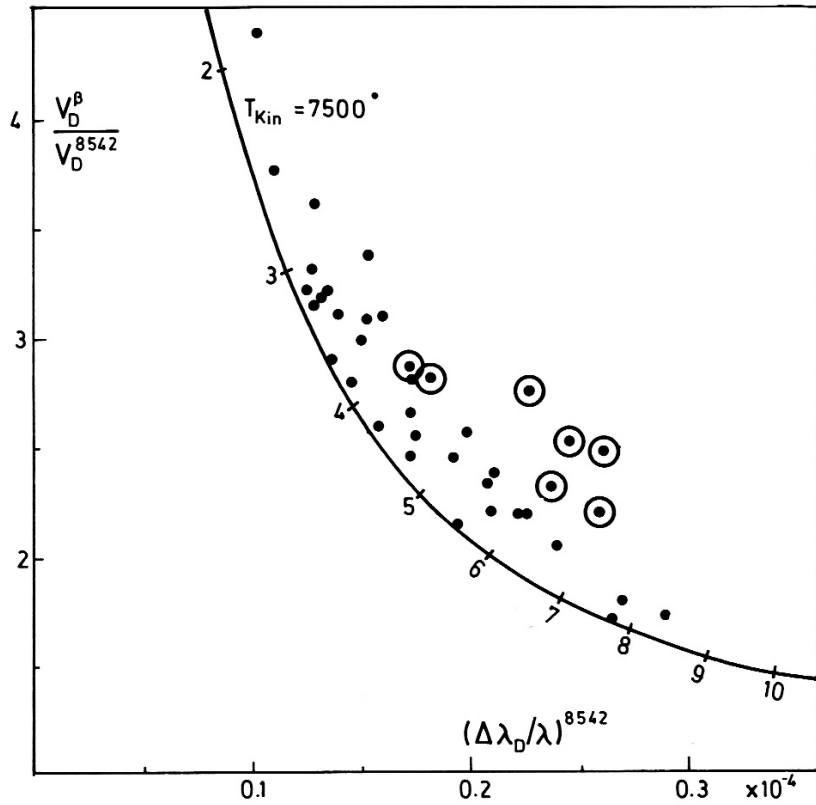


Figure 2. Observed ratio of the reduced width $v_D = \Delta\lambda/\lambda$ of $H\beta$ and Ca II IR vs that of Ca II IR. Solid line: calculated relation for $T_{kin} = 7500 \text{ K}$ and varying non-thermal broadening given as parameter along the curve. Encircled symbols denote emissions with corresponding self-absorbed $H\beta$ profiles.

3. Line Widths

If we suppose that for optically thin prominence emissions, the thermal and non-thermal line broadening constitute the only significant mechanism, we may deduce mean values of the kinetic temperature, T_{kin} , and the non-thermal broadening, v_{nth} from the observed line profiles: those from atoms of small mass (e.g. H β with $\mu = 1$) depend mostly on T_{kin} , while those from atoms with large mass (e.g. Ca with $\mu = 40$) are dominated by non-thermal broadening.

In Figure 2 we give the ratio of the reduced Doppler widths, $v_D = \Delta\lambda_D/\lambda$, for H β and Ca II IR as a function of $v_D(\text{Ca II IR})$. [In the case of non Gaussian profiles $\Delta\lambda_D$ is defined as half width $\Delta\lambda_e$ at I_o/e .] It can be seen that the observations follow the general trend of a calculated curve:

$$c \cdot v_0 = c \cdot \Delta\lambda_D = (2RT_{kin}/\mu + v_{nth}^2)^{-1/2} \quad (1)$$

with parameters $T_{kin} = 7500$ K and $3 \text{ km/s} \leq v_{nth} \leq 8 \text{ km/s}$ adapted to the lower limit of the data. These well agree with those by Hirayama (1978), who obtained $4500 \text{ K} < T_{kin} < 8500 \text{ K}$ and $3 \text{ km/s} < v_{nth} < 8 \text{ km/s}$. Similar values were also deduced by Landman et al. (1977) from their analysis of the widths of H β , He D $_3$ and Ca II IR.

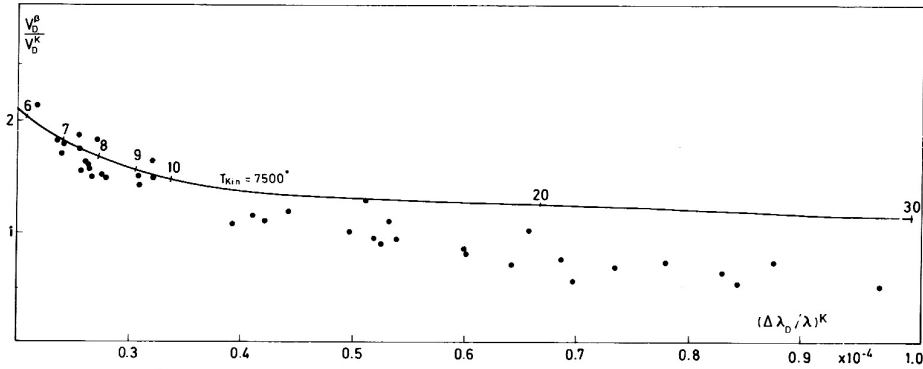


Figure 3. Observed ratio of the reduced width of H β and Ca II K vs that of Ca II K. Solid line: calculated as in Fig. 2.

A corresponding plot for the observed widths of H β and Ca II K (Figure 3) shows stronger deviations from the calculated curve in the sense of additional broadening of the Ca II K lines. This may be due to self-absorption, but also to unresolved macro-shifts, visible in some Doppler-shifted emission ejecta (see also Engvold and Malville, 1977).

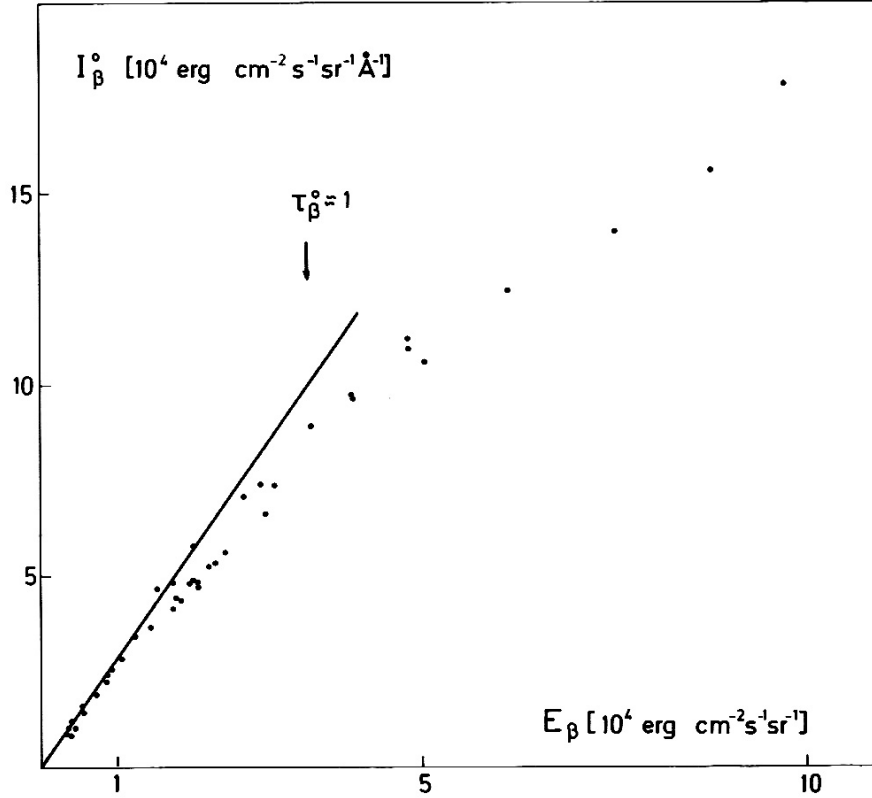


Figure 4. Observed central intensity versus integrated line emission for H β ; solid line: limiting slope corresponding to $\Delta\lambda_D^{min} = 188 \text{ m\AA}$; $E(\tau_\beta = 1)$ from Stellmacher (1969).

4. Emission Relation

The emission relations of Ca II H, K and H α , H β show a branching that depends on the widths of the Ca II lines (Stellmacher 1979). The non-thermal broadening, v_{nth} , widens the profiles and reduces their central intensity, I_0 ; the integrated intensity $E = \int I_\lambda d\lambda$ ('line radiance') remains unchanged, except for the optically thick case.

For an optically thin line with pure Gaussian profile it is $E = I_0 \cdot \Delta\lambda_D \cdot \sqrt{\pi}$. The relation of observed I_0 and E shows for H β (Fig. 4) a smaller scatter than for Ca II IR (Fig. 5). This reflects the strong dependence of the latter on the non-thermal broadening, v_{nth} , which varies by more than a factor of three (cf., Figure 2), whereas H β depends mostly on the (much less varying) T_{kin} . The tight relation of I_0^β and E^β (Figure 4) allows one to use I_0^β as a measure for the total thickness of the prominence (i.e. its number-density).

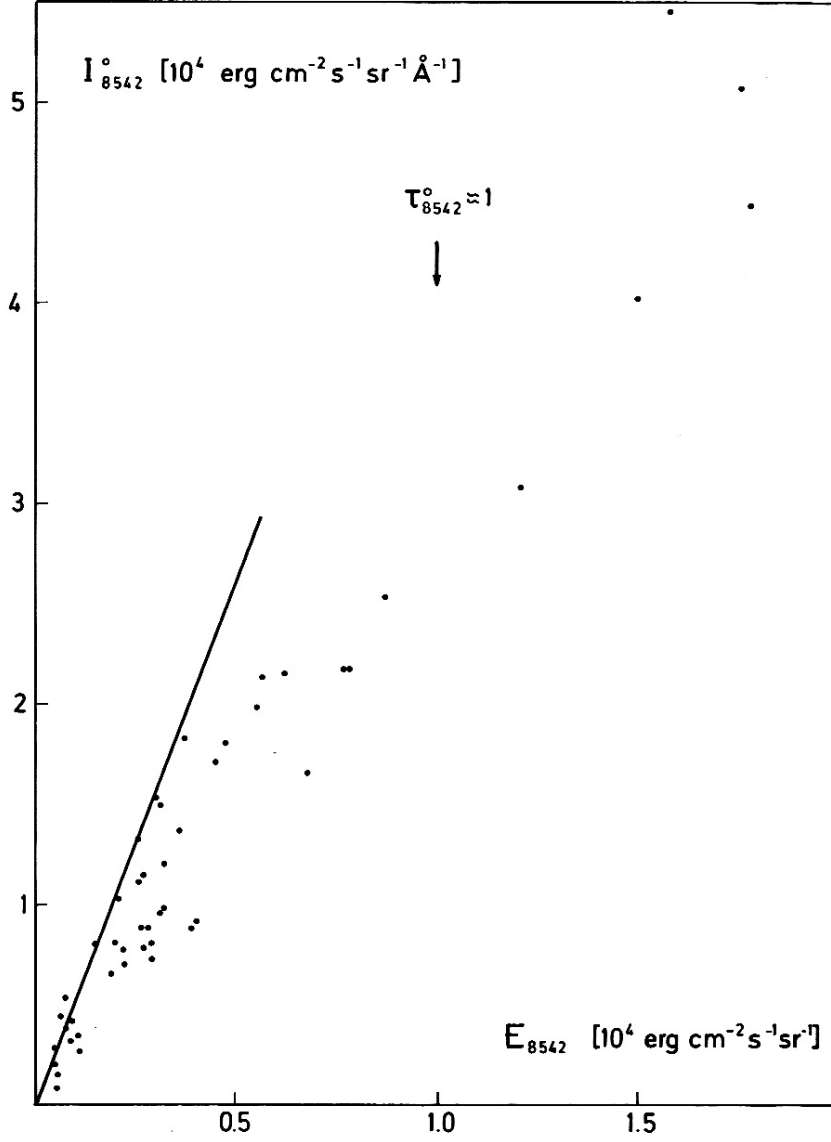


Figure 5. Observed central intensity versus integrated line emission for Ca II IR; *solid line*: limiting slope corresponding to $\Delta\lambda_D^{min} = 105 \text{ m\AA}$; $E(\tau_{Ca} = 1)$ from Landman (1979).

The steepest slopes in the two plots correspond to narrowest reduced widths $[\Delta\lambda_D^{min}/\lambda]_{H\beta} = 3.87 \cdot 10^{-5}$ and $[\Delta\lambda_D^{min}/\lambda]_{CaIR} = 1.23 \cdot 10^{-5}$, respectively. Inserted into formula 1 these give $T_{kin} = 7570 \text{ K}$ and $v_{nth} = 3.6 \text{ km/s}$. We note that for Ca II IR our relation I_0 versus E well agrees with the one given Landman (1979).

The bending in the observed relation I_0 vs E (Fig. 4) shows that saturation becomes effective for the $H\beta$ emission. For an estimate of the $H\beta$ optical thickness, we use the $H\alpha$ optical thickness, $\tau_\alpha^0 = 3.6$, which Stellmacher (1969) gives for $E\beta \approx 1.7 \cdot 10^4$ erg/(s cm² ster). With $\tau_\alpha^0/\tau_\beta^0 = (\lambda_{32} \cdot f_{32})/(\lambda_{42} \cdot f_{42}) = 7.25$, we deduce a corresponding $H\beta$ optical thickness of $\tau_\beta = 0.5$. Based on this value, we can now determine for $\tau_\beta = 1$ a mean $H\beta$ radiance $E_\beta = 3.5 \cdot 10^4$ erg/(s cm² ster). [Similar values are obtained on the basis of the analysis by Landman and Mongillo (1979).] The widths of the seven broadest $H\beta$ lines in Figure 4 with $E_\beta \geq 5 \cdot 10^4$ erg/(s cm² ster), where saturation becomes important, are encircled in Figure 2.

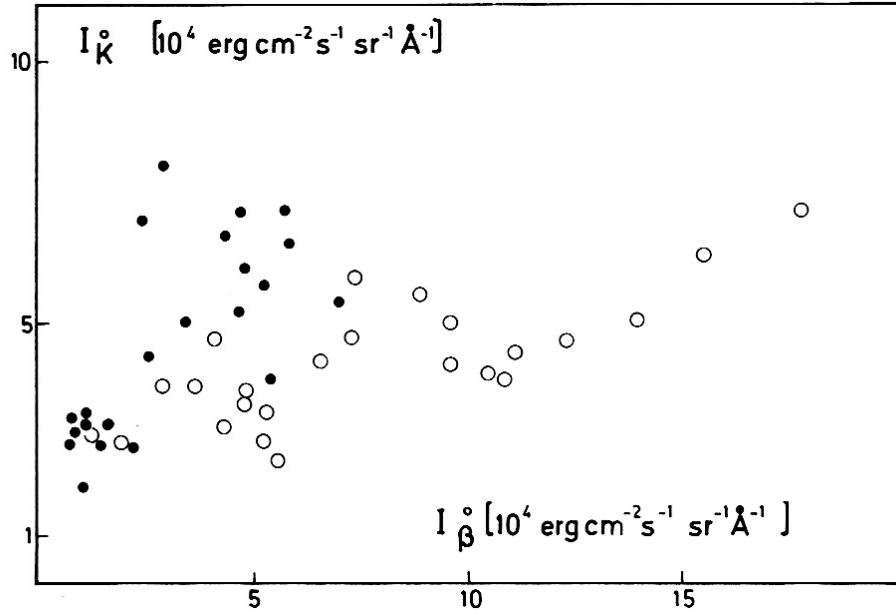


Figure 6. Observed relation of the central intensity of Ca II K and $H\beta$; open circles denote broad Ca II K profiles with $R^K < 1.45$).

Figure 6 shows the central intensity I_0 of the observed Ca II K line versus that of the corresponding $H\beta$ line, (the latter giving the total prominence thickness as argued above). The observed relation can be separated into two distinct branches defined by the ratio of their reduced Doppler width v_D^β/v_D^K from Figure 3. The upper branch (full dots in Fig. 6) contains data with $v_D^\beta/v_D^K \geq 1.45$, which are characteristic for narrow Ca II K profiles ($\Delta\lambda_D/\lambda < 0.3 \cdot 10^{-6}$ in Fig. 3). The lower branch (open circles in Fig. 6) contains data with $v_D^\beta/v_D^K \leq 1.45$, which are characteristic for broad the Ca II K profiles in Figure 3. Hence, the difference in the central Ca II K intensity for a given I_0^β reflects their strong sensitivity to non-thermal broadening.

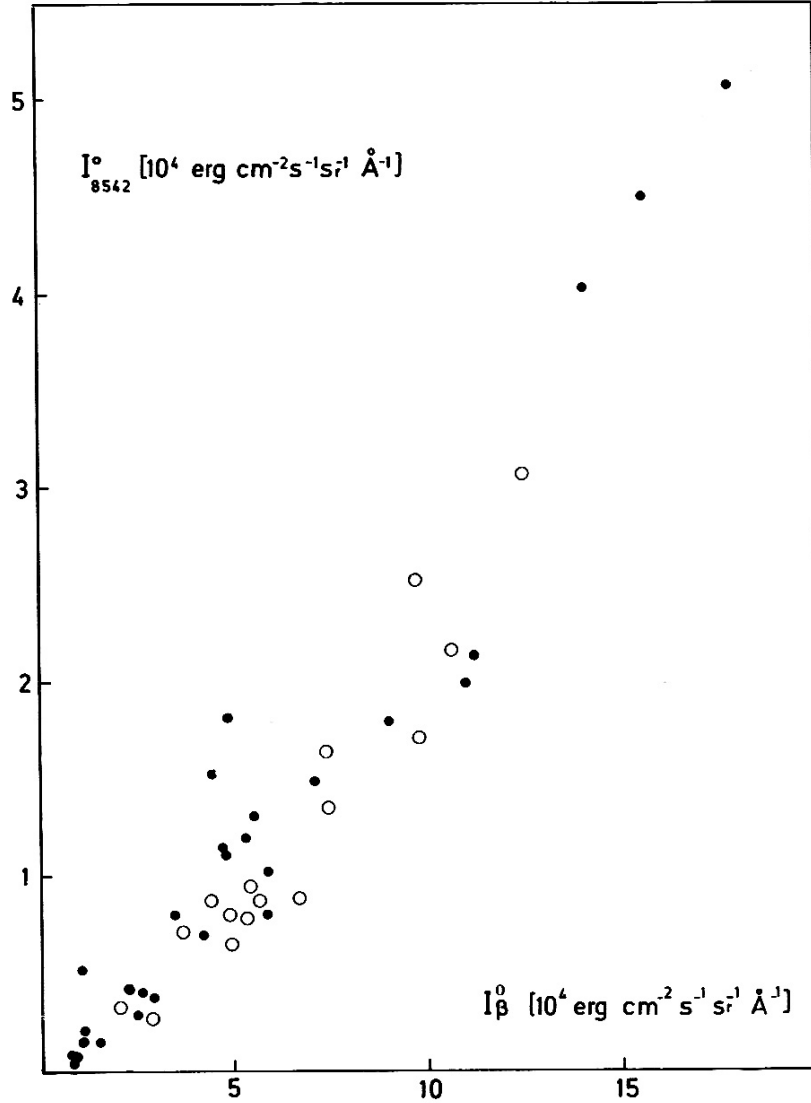


Figure 7. Observed relation of the central intensity of Ca II IR and H β ; open circles denote broad Ca II IR profiles with $R^K < 2.5$).

A similar relation, but for the observed Ca II IR and H β line is shown in Figure 7. Here, the branching is much less pronounced. For optical thin layers with central intensities $I_{\beta} \leq 10 \cdot 10^4 \text{ erg}/(\text{s cm}^2 \text{ ster } \text{\AA})$ in Figure 7, we find a slight indication that narrow Ca II IR profiles with $v_D^{\beta}/v_D^{IR} \geq 2.5$ (cf., Fig. 2) tend to follow the upper part of the relation (full dots in Figure 7).

5. Conclusions

We confirm that the branching in the Ca II versus Balmer emission correlates with the non-thermal line broadening, v_{nth} . The importance of that parameter for the transfer problem of the Ca II lines was discussed by Heasley and Milkey (1978). Comparison of their calculated relation $E(\text{Ca II K})$ vs $E(\text{Ca II H})$ with observations by Landman and Illing (1977) gave small values $v_{nth} \leq 2$ km/s. Stellmacher (1979) obtained $2 \leq v_{nth} \leq 4$ km/s, being compatible with values he obtained from higher Balmer lines and He D₃.

The line-width method (through Equation (1)) may be reliable, if the widths of the hydrogen, helium and metal lines give single values for T_{kin} and v_{nth} . However, the time variation of the prominence structure ('threads') suggests that *large scale motions may affect a line broadening in addition to the thermal and non-thermal velocities.*

Corresponding calculations have been carried out by Kawaguchi (1966) for the Balmer line profiles. He assumed different laws for the distribution of the thread velocities (independent of the position along the line of sight) and constant thermal and non-thermal (Maxwellian) broadening within each optically thin thread. He obtained (apart from a Gaussian distribution law, which again results in Gaussian profiles) non-Gaussian shapes for the additional line broadening.

Hence, *the structure of the prominence itself influences the line width and the total emission by convolution of the internal Maxwellian broadening with the (macro-) velocity distribution function of threads along the line of sight.* Side-on and edge-on observations of prominences may then be spectroscopically distinct; a possible example was discussed by Landman and Illing (1977) in context with the branching of their Ca II K versus Ca II IR emission relation. Similarly, differences in $E(\text{Ca II K})/E(\text{H}\alpha)$ ratio found by Engvold et al. (1978) between ordinary prominence structures and edge structures with 'ejecta' may be related to such a modified line broadening.

References

- Brückner, G.: 1961, Z. f. Astrophys. 51, 187
 Engvold, O.: 1978, Solar Phys. 56, 87.
 Engvold, O. and Malville, J. M.: 1977, Solar Phys. 52, 369.
 Engvold, O., Malville, J. M., and Livingston, W.: 1978, Solar Phys. 60, 57,
 Heasley, J. N. and Milkey, R. W.: 1978, Astrophys. J. 221, 677.
 Hirayama, T.: 1978, in E. Jensen. P. Maltby, and F. Q. Orrall (eds.), Physics of Solar Prominences', IAU Colloq. 44, 4.
 Kawaguchi, I.: 1966, Publ. Astron. Soc. Japan 18, 362.
 Labs, D. and Neckel, H.: 1968, Z. Astrophys. 69, 1.
 Landman, D. A. and Illing, R. M. E.: 1977, Astron. Astrophys. 55, 103.
 Landman, D. A., Edberg, S. J. and Laney, C. D.: 1977, Astrophys. J. 218, 888.

- Landman, D. A. and Mongillo, M.: 1979, *Astrophys. J.* 230, 581.
Landman, D. A.: 1979, preprint.
Stellmacher, G.: 1969, *Astron. Astrophys.* 1, 62.
Stellmacher, G.: 1978, in E. Jensen, P. Maltby, and F. Q. Orrall eds., *Physics of Solar Prominences*, IAU-colloq. 44, 33.
Stellmacher, G.: 1979, *Solar Phys.* 61, 61.
White, O. R. and Suemoto, Z.: 1968, *Solar Phys.* 3, 523.
Wiehr, E., Wöhl, H., and Wittmann, A.: 1980, *Solar Phys.* 68, 207.